

PAPER • OPEN ACCESS

## Effects of heat treatment on microstructures of a Re-containing Ni-based single crystal superalloy

To cite this article: J Zhang *et al* 2019 *IOP Conf. Ser.: Mater. Sci. Eng.* **605** 012017

View the [article online](#) for updates and enhancements.

# Effects of heat treatment on microstructures of a Re-containing Ni-based single crystal superalloy

J Zhang<sup>1</sup>, L Q Gao<sup>1,2,\*</sup>, Y F Liu<sup>3</sup>, J X Zhao<sup>1</sup> and X T Zhang<sup>1</sup>

1. Science and Technology on Advanced High Temperature Structural Materials Laboratory, Beijing Institute of Aeronautical Materials, Beijing 100095, P. R. China

2. School of Mechanics, Civil Engineering and Architecture, Northwestern Polytechnical University, Xi'an, 710072, P. R. China

3. AECC Sichuan Gas Turbine Establishment, Chengdu 610500, P. R. China

E-mail: [zhangjian620@foxmail.com](mailto:zhangjian620@foxmail.com); [lqgao0214@163.com](mailto:lqgao0214@163.com); [824300948@qq.com](mailto:824300948@qq.com); [455531944@qq.com](mailto:455531944@qq.com); [www.529881022@qq.com](http://www.529881022@qq.com).

\* Corresponding Author: [lqgao0214@163.com](mailto:lqgao0214@163.com)

**Abstract.** Effects of heat treatment on microstructures of a Re-containing single crystal superalloy have been investigated. The results showed that  $(\gamma+\gamma')$  eutectic in as-cast alloy is practically dissolved with solution heat treatment, and the degree of segregation is distinctly decreased. The size, morphology and distribution of  $\gamma'$  phase are mightily affected by the first-stage ageing treatment temperature. When the first-stage ageing treatment temperature lower than 1160 °C, the shape of the  $\gamma'$  phase is cubic. But the  $\gamma'$  phase shape is transformed to sphericity when the temperature higher than 1180 °C. The  $\gamma$  phase channel width is significantly increased, and the fine  $\gamma'$  phase precipitated in the  $\gamma$  phase matrix channel.

**Key words.** Superalloy; Heat treatment; Microstructures;  $\gamma$  phase matrix channel

## 1. Introduction

Nickel-based single crystal superalloy is the key material for advanced aeroengine turbine blades and ground gas turbine blades. Monocrystalline alloys are prepared by selective crystallization or seed crystallization growing in dendrite orientation. Due to solute redistribution during the solidification process, a large amount of Al, Ta and other elements forming the  $\gamma'$  phase will be enriched in the dendrite cores of as-cast alloys, while Re, W, Mo and other elements forming the  $\gamma$  phase will be enriched in the dendrite cores [1,2]. The solidification segregation of cast superalloy results in the low degree of alloying in some parts of the alloys, which decreases the properties of the alloys; while the high degree of alloying in other parts promotes the precipitation of TCP phase and reduces the properties of the alloys [3]. Meanwhile, during the solidification and cooling process of single crystal superalloy, coarser and inhomogeneous  $\gamma'$  phases are precipitated, and there are  $(\gamma+\gamma')$  eutectics in the interdendritic region, which can also significantly reduce the mechanical properties of the alloys [4].

The purpose of heat treatment of nickel-based single crystal superalloy is to reduce dendritic segregation during the directional solidification process, to adjust the morphology and size of the  $\gamma'$  phase in single crystal superalloy, and to improve the mechanical properties of the alloys. Heat treatment process usually includes solution treatment and aging treatment. The main function of solution treatment is to solute all or most of the coarse  $\gamma'$  phase and  $\gamma/\gamma'$  eutectic in as-cast alloys,



thereby improving the homogeneity of the structure and reducing the solidification segregation [5]. In order to further develop the performance potential of single crystal alloys, two-stage aging heat treatment is usually adopted after solution heat treatment to improve the properties of the alloys. It is generally believed that the first ageing treatment is a process of growth of  $\gamma'$  phase and the second ageing treatment is a process of increasing the square degree of  $\gamma'$  phase [6].

Persistent creep rupture is one of the most important mechanical properties of nickel-based single crystal alloys, and has been extensively investigated. The  $\gamma'$  phase is the most important strengthening phase, and its shape, size, volume fraction and distribution determine the creep rupture properties of the alloy [7]. At present, there are still many disputes about the type of organization is beneficial to creep properties and how the organization affects creep properties. And P. Caron and T. Khan [8] studied CMSX-2 and found that the best creep properties of the alloy can be obtained by choosing appropriate ageing treatment process, so that the  $\gamma'$  phase in the alloy eventually becomes a regular square with a size of about  $0.45\mu\text{m}$ . However, Mackay and Ebert [9] observed different situations in Alloy 143, and the creep properties of the alloy are improved when the size is refined from  $0.44\mu\text{m}$  to  $0.15\mu\text{m}$ . At the same time, Murakumo et al. [10] studied that as the main strengthening phase, the optimum morphology of  $\gamma'$  phase in unequal alloys is different, so it is necessary to study each alloy in detail.

By adding Re and other refractory elements in the second and third generation single crystal alloys, the creep rupture properties of the alloys are significantly improved [2]. However, Re is a strong negative segregation element and promotes the segregation of other elements, resulting in the decrease of the uniformity of the alloy structure. Therefore, the research on heat treatment process of single crystal alloys containing Re becomes more and more vital. The heat treatment of single crystal superalloy has been deeply studied in the United States and Russia, and the precipitation dissolution and the number and distribution of strengthening phases in the alloys have been systematically researched, and different heat treatment systems are recommended for the same alloy to adapt the requirements of different working conditions [11,12]. At present, the research on the heat treatment process of single crystal superalloy is not systematic in China, especially the research of the content, size, morphology and homogeneity of the strengthened phase on the rupture properties of the alloys containing Re is not much.

DD11 alloy is the second-generation nickel-based single crystal superalloy containing Re developed independently by Beijing Institute of Aeronautical Materials in recent years, and its content of Re is 3 wt%, and it is mainly used to manufacture advanced aeroengine turbine blades [1]. In this research, the content, size and morphology of the strengthened phase of the alloys under distinct ageing heat treatment conditions are investigated, and the relationship between microstructures and temperatures is discussed.

## 2. Experimental materials and methods

In order to study the effect of heat treatment on the structure and rupture properties of nickel-based single crystal superalloy, the DD11 alloy developed by Beijing Institute of Aeronautical Materials is chosen as the base alloy, and its chemical composition (wt,%) is presented in Table 1. In HRS directional solidification furnace, single crystal rods with [001] orientation of 15 mm in diameter and 150 mm in length are prepared by Spiral crystal selection, and the pulling speed is 3 mm/min during directional solidification. The orientation of single crystal is determined by backscattering Laue method, and the rod whose growth direction deviated from [001] direction is less than 10 degrees is selected as the experimental material. On the NETZSCH STA449C differential thermal analyzer (DSC), the phase transformation temperature of the alloy is measured at a rate of  $10^\circ\text{C}/\text{min}$  from  $1000^\circ\text{C}$  to  $1430^\circ\text{C}$ . According to the principle of eliminating eutectic, reducing dendrite segregation and avoiding primary melting, the solid solution heat treatment system is determined. Under this system, six different temperatures are selected for the first-stage ageing treatment. Then the same second-stage aging treatment is carried out for the test sample. The first-stage aging treatment temperature is  $1100^\circ\text{C}$ ,  $1120^\circ\text{C}$ ,  $1140^\circ\text{C}$ ,  $1160^\circ\text{C}$ ,  $1180^\circ\text{C}$  and  $1200^\circ\text{C}$ , and after holding for 4 hours, air-cooling is

carried out. The second-stage aging treatment is air cooling after holding for 32 hours at 870 °C (Table 2). After different heat treatments, the alloy is processed into standard specimens with gauge diameter of 5 mm, gauge length of 25 mm and total length of 66 mm. The high temperature endurance test is carried out at 1100 °C/140 MPa and 980 °C/250 MPa, and the endurance life is determined by the average values of three specimens. The corrosive solution of metallographic specimens is 1% HF + 33% HNO<sub>3</sub> + 33% CH<sub>3</sub>COOH + 33% H<sub>2</sub>O (vol.%). Microstructure morphologies at low and high power are observed by using optical microscopy (OM) and secondary electron mode of SUPRA 55 field emission scanning electron microscopy (FE-SEM). In this work, the volume fraction of  $\gamma'$  phase is measured by point analysis method, and the size of  $\gamma'$  phase is measured by Image-Pro software. The same specimens are counted by 6 to 8 photos.

**Table 1.** Chemical composition of the DD11 alloy (Wt. %).

Element	Al	Cr	Ta	W	Co	Mo	Re	C	Hf	Ni
Mass fraction/%	6.0	4.0	7.0	7.0	8.0	2.0	3.0	0.01	0.15	surplus

The elemental solidification segregation coefficient  $S_i$  and the solidification segregation coefficient  $S_i$  of as-cast alloy after solution heat treatment are measured by JEOL JXA-8800R electron probe (EPMA).

Elemental solidification segregation coefficient  $S_i$  can be expressed as:

$$S_i = C_{\text{dendrite}}^i / C_{\text{interdendrite}}^i \quad (1)$$

In the formula, the sum is the concentration of element  $i$  in the dendrite cores and between the interdendrites.  $S_i > 1$  indicates that the alloy element  $i$  segregates to the dendrite cores, while  $S_i < 1$  indicates that the alloy element  $i$  segregates to the interdendrites.

**Table 2.** Solid Solution and Aging Heat Treatment Systems of Experimental Alloys.

Specimens	Solution treatment	First-stage aging treatment	Second-stage aging treatment
A		1100 °C/4h, AC	
B	( 1290/2h+	1120 °C/4h, AC	
C	1300 °C/2h	1140 °C/4h, AC	
D	+1310 °C/2h)	1160 °C/4h, AC	870 °C/32 h, AC
E	+1320 °C/6h	1180 °C/4h, AC	
F		1200 °C/4h, AC	

### 3. Experimental results

#### 3.1. Microstructure and transformation temperature of as-cast alloy

Fig.1 (a) is Optical microscopy image of as-cast alloy. It can be seen from the graph that the structure of the alloy presents typical dendrite morphology. The primary dendrite spacing is 340  $\mu\text{m}$ . The white brightness contrast between interdendrites of the alloy is  $\gamma/\gamma'$  eutectic structure, and the volume

fraction of the eutectic is about 6%. Fig.1 (b) and Fig.1 (c) are morphologies of dendrite cores and interdendritic morphologies of as-cast alloys respectively. It can be seen that the dendrite cores  $\gamma'$  phase are all butterfly-shaped with uneven size and great difference. In addition, the  $\gamma'$  phase is relatively small and the average size of the  $\gamma'$  phase is about 400nm. The interdendritic  $\gamma'$  phase size is larger, the cubic degree is better than the dendrite cores and the average size of the  $\gamma'$  phase is about 720nm.

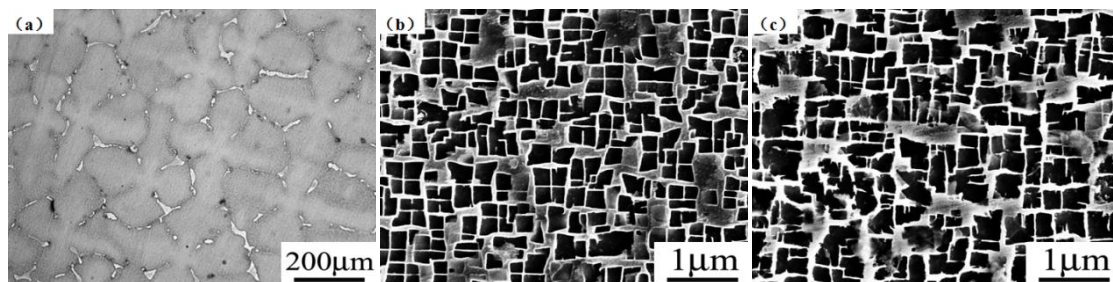


**Fig. 1.** Microstructures of as-cast alloys: (a) Optical microscopy image; (b) SEM image of dendrite cores; (c) SEM image of interdendrites.

Fig. 2. shows the DSC heating curve of as-cast alloys. There are three endothermic reactions on DSC heating curve. The first endothermic peak is due to the solid solution of the  $\gamma'$  phase between dendrite cores and interdendrites, and the dissolution temperature of the twisted phase of the alloy is about 1250°C. The second endothermic peak is the melting temperature of  $\gamma/\gamma'$  eutectic. The eutectic dissolution temperature measured by DSC is about 1351°C. The third endothermic peak is the liquidus of the alloy, which is about 1404°C. At the same time, the solid phase line is the intersection temperature of the endothermic peak tangent and the baseline, and the solid phase line of the alloy is about 1368°C.

In DSC measurements, a small amount of liquids did not fully solidify in a wide temperature range during the late solidification stage, and the thermal effect of these phase transitions is very weak. Therefore, there is a certain deviation between the phase transformation temperature measured by DSC curve and the actual phase transformation temperature of the alloy. In order to determine the actual "heat treatment window", under the guidance of the results of differential thermal analysis, the rapid water-cooled structure of the alloy sample after holding at different temperatures (1300°C ~1350°C) is observed, that is, the eutectic dissolution temperature and initial melting temperature of the alloy are determined by metallographic method, and a reasonable solution treatment system is finally worked out. Fig. 3. shows the variation of volume fraction of eutectic dissolution and initial melting with solution temperature. As can be seen from Fig.3, the eutectic structure gradually dissolves with the increase of solution temperature, and the eutectic structure completely dissolves when heated to 1315°C. When the solution temperature reaches 1335°C, the initial melting occurs in the alloy, and the fraction of the initial melting volume increases gradually with the increase of heating temperature. The temperature range between solution  $\gamma'$  phase temperature and initial melting temperature of the alloy is usually called "heat treatment window". Solution treatment temperature should be selected in the heat treatment window to ensure that the  $\gamma'$  phase can be dissolved into the  $\gamma$  phase without initial melting, eliminate eutectic ( $\gamma+\gamma'$ ) and achieve homogenization of alloy elements. As can be seen from Fig.3, the "heat treatment window" of the alloy is 1315°C~1330°C. The lowering of initial melting temperature obtained by metallographic method by 10°C is set as the highest solid solution temperature, which can not only improve the efficiency of solid solution heat treatment to the greatest extent, but also prevent the initial melting of alloys caused by temperature fluctuation during the heating process of heat treatment furnace. Stepped solid solution heat treatment method is adopted. By comparing the structures after different time solid solution treatment, considering the time and

effect of solid solution, the solid solution heat treatment system as listed in the Table 2 is finally determined.

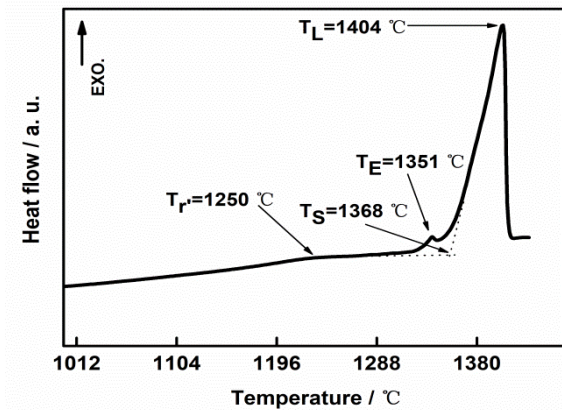


**Fig.2.** DSC heating results of the as-cast alloy.

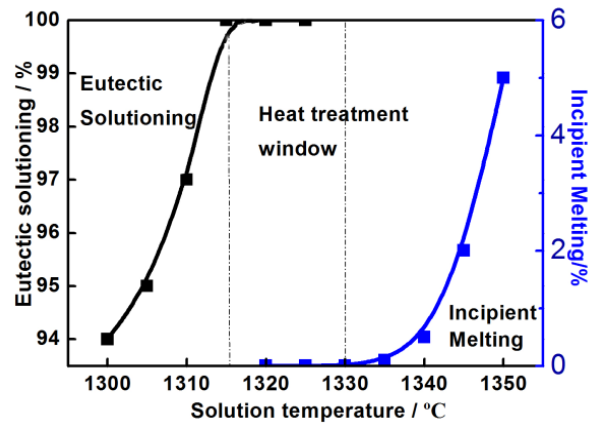


**Fig.3.** Changes of volume fraction of eutectic dissolution and initial melting with the increasing of solution temperature.

### 3.2. Microstructure after alloy solution heat treatment

Fig. 4 (a) shows the microstructure of the alloy after solution heat treatment. It can be seen that the eutectic of the  $\gamma/\gamma'$  two-phase of the alloy has been completely eliminated. But due to the high content of refractory elements such as Re, W and Ta in the alloy, dendrite cores patterns can still be observed in the solution heat treatment microstructure. Fig. 4(b) and 4(c) show the scanned tissue of the dendrite cores and interdendritic region after alloy solution heat treatment. It can be seen that the shape of the  $\gamma'$  phase in the dendrite cores, and inter-dendritic region after alloy solution heat treatment is more regular and average than the as-cast state and the size of the  $\gamma'$  phase becomes more finer. According to statistics, the average size of the dendrite cores  $\gamma'$  phase is about 80 nm, and the average size of the interdendrites  $\gamma'$  phase is about 120 nm.

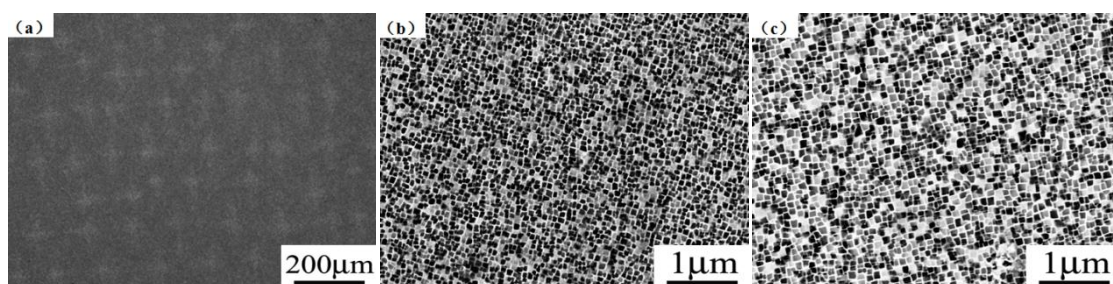


**Fig. 4.** Microstructures of solid solution alloy: (a)Optical microscopy image; (b) SEM image of dendrite cores; (c) SEM image of interdendrites.

Fig. 5. is a comparison of the segregation coefficients of the elements before and after the solution heat treatment of the alloy. It can be seen that the degree of segregation of all alloying elements after solution heat treatment has been reduced distinctly. The segregation type of each alloying element did not change, Re and W are still negative segregation elements, and Mo, Al and Ta are still positive segregation elements. After solution heat treatment, Re is still the most serious negative segregation element. The segregation coefficient is changed from 1.87 to 1.46; W is a more serious negative segregation element. The segregation coefficient is changed from 1.60 to 1.22; Ta is the most serious



positive segregation element. The segregation coefficient is changed from 0.65 to 0.87; Al and Mo are weaker positive segregation elements, and the segregation ratio is closer to 1 after solution heat treatment.

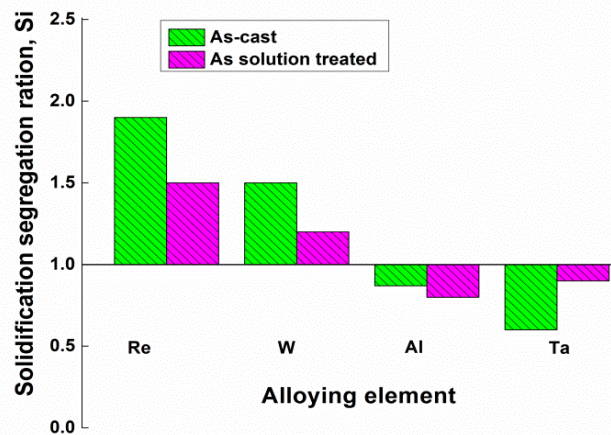


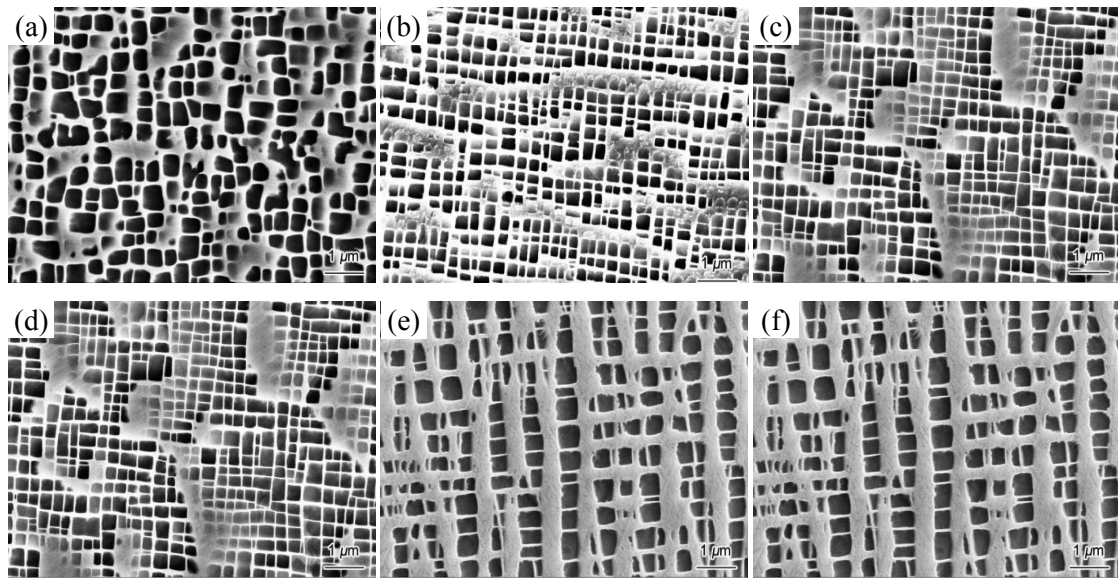
**Fig. 5.** Comparison of segregation of various elements before and after solution heat treatment.

Therefore, the high temperature solution heat treatment significantly improves the uniformity of the microstructure and composition of the dendrite cores and interdendritic region of the alloy. It significantly reduces the difference between the precipitation strengthening and the solid solution strengthening effect in different region of the alloy, thereby improving the dendrite cores and branches of the alloy. The continuity and uniformity of the inter granular strength play a significant role in the improvement of the mechanical properties of the alloy.

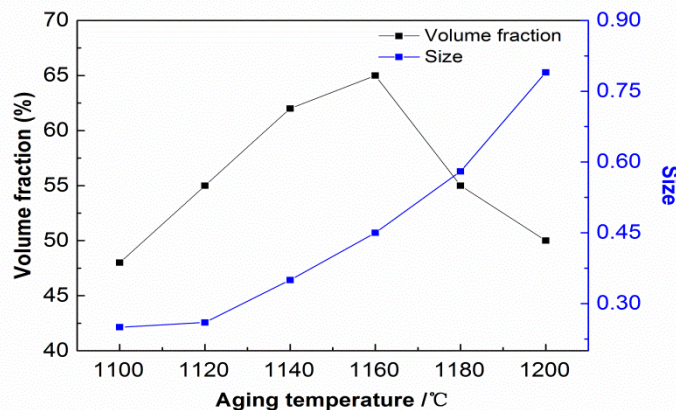
### 3.3. Alloy after aging heat treatment

Fig. 6. shows the typical microstructure of the alloy dendrite cores after different the first-stage aging treatment ((1100°C~1200°C)/4h, AC), and after the same secondary aging treatment (870°C/32h, AC). From the aspect of the phase of the  $\gamma'$  phase, when the alloy aging temperature is 1100°C, the cubicity of the  $\gamma'$  phase is poor. The cubicity of the  $\gamma'$  phase is gradually increased and the arrangement of the  $\gamma'$  phase is more neat when the alloy aging temperature is 1120°C and 1140°C. When the aging treatment temperature is 1160°C, the alloy cubicity begins to decrease. The sharp corners of the  $\gamma'$  phase begin to dissolve, making the cube smooth. The morphology of the  $\gamma'$  phase is similar to that of the spherical shape and the precipitation of the fine  $\gamma'$  phase is present in the wide  $\gamma$  matrix channel when the aging treatment temperature is 1180°C and 1200°C. When the aging treatment temperature is 1100°C~1140°C, the average size of the  $\gamma'$  phase becomes insignificant and approximately 0.32 $\mu$ m. However, when the aging temperature exceeds 1160°C, the average size of the  $\gamma'$  phase gradually increases and the effective temperature is 1200°C, the  $\gamma'$  phase coarsening becomes serious. The average size of the  $\gamma'$  phase is 0.8 $\mu$ m. With the increase of the first-age aging temperature, the volume fraction of the strontium between the dendrite cores and the interdendritic region increased first and then decreased, reaching a peak at 1140°C and 1160°C.

Fig. 7. shows the changes in the size and volume fraction of the dendritic core  $\gamma'$  phase of the alloy after different aging heat treatments. When the aging temperature is 1100 °C to 1140 °C, and the average size change of the  $\gamma'$  phase is not significant, about 0.32 $\mu$  m. When the aging temperature exceeds 1160 °C, the average size of the  $\gamma'$  phase gradually increases, the effective temperature is 1200 °C, the  $\gamma'$  phase coarsens seriously, and the average size of the  $\gamma'$  phase reaches 0.8  $\mu$ m. As the first-stage aging treatment temperature increases, the volume fraction of the dendritic core  $\gamma'$  phase increases first and then decreases, reaching a peak at 1160 °C (Fig. 7.), and the peak value is about 66%.



**Fig. 6.** Microstructure of the alloy dendrite cores after different the first-stage aging treatment: (a) 1100°C, (b) 1120°C, (c) 1140°C, (d) 1160°C, (e) 1180°C and (f) 1200°C.



**Fig. 7.** Changes in size and volume fraction of the dendritic core  $\gamma'$  phase of the alloy after different aging heat treatments.

#### 4. Discussion

The single-phase solid solution is firstly precipitated from the liquid phase when the nickel-based single crystal superalloy is solidified. The single-phase solid solution is dendritic growth and the high melting point elements such as Re and W are enriched to in dendrite cores At the same time, elements such as Al and Ta are concentrated in the liquid phase between the interdendritic region. As the liquid phase between the interdendrites solidifies, the concentration of the solute in a small amount of the remaining liquid phase reaches the eutectic point, forming the  $\gamma/\gamma'$  eutectic. The content of as-cast eutectic can reflect the degree of solidification segregation [1]. In this work, about 6% of the  $\gamma/\gamma'$  eutectic exists in the as-cast microstructure (Fig. 1. ), and as-cast segregation is also severe, and the solidification segregation coefficient of Re reaches 1.87 (Fig. 5. ).

Pretreatment of as-cast alloy by 1290°C/2h+ 1300°C/2h+1310°C/2h can reduce the degree of segregation of low melting point elements in the interdendritic region, and avoid the initial melting of the alloy. Subsequently, the high temperature solution treatment at 1320°C/6h is carried out, which makes the  $\gamma/\gamma'$  eutectic structure and the coarse  $\gamma'$  phase in the as-cast alloy completely dissolve into



the  $\gamma$  matrix. Meanwhile, the insoluble alloying elements are sufficiently diffused at a high temperature which reduces the solidification segregation of the alloy and increases the degree of homogenization of the alloy composition (Fig. 5. ). In the subsequent solid solution air cooling process, a large number of fine nanoscale  $\gamma'$  phase particles are precipitated from the supersaturated  $\gamma$  matrix. That is because the elements such as Ta and Al in the interdendritic region are still higher than the dendrite cores. Ta and Al are the main forming elements of the  $\gamma'$  phase and size of the  $\gamma'$  phase between the interdendritic region after solution heat treatment is significantly larger than that of the dendrite cores (Fig 4(b) and (c)). Wang et al. [13] believed that the fine  $\gamma'$  phase precipitated after solid solution maintained a coherent interface with the  $\gamma$  matrix. At the same time, since the cubic  $\gamma'$  phase precipitated is small in size and large in number and there are many interfaces of  $\gamma'/\gamma$  two phases, so there is a large interfacial energy and a certain degree of lattice strain energy in the alloy.

During the first-stage aging treatment of the alloy, the super-saturated  $\gamma'$  phase particles in the alloy continue to grow under the joint action of the coherent interface strain energy. During the aging treatment period from 1100°C to 1140°C, the morphology of the  $\gamma'$  phase is limited by the interfacial energy and coherent interface strain energy between the two phases. The  $\gamma'$  phase does not grow excessively. The  $\gamma'/\gamma$  phase maintains a coherent interface. The interaction of the interfacial energy and the coherent interface strain energy causes the  $\gamma'$  phase to grow into a cubic shape, as shown in (Fig.6(a)~(c)). When the temperature is improved, the  $\gamma'/\gamma$  phase is no longer flat, which indicates that the  $\gamma'/\gamma$  two-phase coherent interface disappears and the strain energy is weakened. Therefore, under the action of the interface energy, the  $\gamma'$  phase can be promoted to grow into a spherical or thick strip-like morphology (Fig. 6(e)~(f)).

## 5. Conclusion

The alloy in as-cast is exhibited a typical dendrite structure and there are approximately 6% the  $\gamma/\gamma'$  eutectic between the interdendritic region. The gold liquidus and solidus temperatures of the alloy are 1404°C and 1368°C respectively. The  $\gamma'$  phase solid solution temperature is 1250°C.

The range of solid solution heat treatment of the alloy is 1315°C~1330°C. After 1320°C/6h of solid solution heat treatment, the segregation of the alloy elements becomes alleviated. The  $\gamma/\gamma'$  eutectic is basically eliminated and the fine  $\gamma'$  phase is precipitated in the solid solution and air cooling process.

As the first-stage aging treatment temperature increases, the size of the  $\gamma'$  phase gradually increases. The volume fraction of the  $\gamma'$  phase first increases and then decreases. The cubicity of the  $\gamma'$  phase decreases when the aging treatment temperature reaches or exceeds 1160°C. The  $\gamma$  matrix channel becomes significantly coarsened and the fine  $\gamma'$  phase is precipitated in the channel when the first-stage treatment aging temperature are 1180°C and 1200°C.

## Acknowledgements

This work was supported by from the National Natural Science Foundation of China (Grant No.51605386) and the AECC Sichuan Gas Turbine Establishment. These supports are gratefully acknowledged.

## References

- [1] Y S Zhao, J Zhang, Y S Luo, et al. Effect of Hf on high temperature low stress rupture properties of a second generation Ni-based single crystal superalloy DD11[J]. Acta Metall Sin, 2015(10): 1261-1272.
- [2] W S Waltson, K S O'Hara, E W Ross, et al. René N6: Third generation single crystal superalloy. Superalloy 1996. Warrendale, PA, 1996: 27-34.
- [3] W S Waltson, Schaeffer, J C, W H Murphy. A new type of microstructural instability in superalloy - SRZ. Superalloy 1996. Warrendale, 1996: 9-18.
- [4] Y H Kong, Q Z Chen, Q Z Knowles. Effects of minor additions on microstructure and creep performance of RR2086 SX superalloy. Journal of Materials Science, 2004, 39(23): 6993-7001.

- [5] G Liu, L Liu, S X Zhang, et al. Effects of Re and Ru on microstructure and segregation of Ni-based single-crystal superalloy[J]. *Acta Metall Sin*, 2012, 48(7): 845-852.
- [6] B C Wilson, G E Fuchs. The effect of composition, misfit, and heat treatment on the primary creep behavior of single crystal nickel base superalloy PWA 1480 and PWA 1484. Warrendale: Minerals, Metals & Materials Soc, 2008:
- [7] P Caron, T Khan, Y Ohta, et al. Creep deformation anisotropy in single crystal superalloy. *Superalloy 1988*, 1988: 215-224.
- [8] P K Caron. Improvement of creep strength in a nickel-base single-crystal superalloy by heat treatment. *Materials Science and Engineering A*, 1983, 61(2): 173-184.
- [9] R Mackay, L Ebert. The development of  $\gamma$ - $\gamma'$  lamellar structures in a nickel-base superalloy during elevated temperature mechanical testing. *Metallurgical and Materials Transactions A*, 1985, 16(11): 1969-1982.
- [10] T Murakumo, T Kobayashy, Y Koizumi, et al. Creep behaviour of Ni-base single-crystal superalloy with various  $\gamma'$  volume fraction. *Acta Materialia*, 2004, 52(12): 3737-3744.
- [11] G E Fuchs. Improvement of creep strength of a third generation, single-crystal Ni-base superalloy by solution heat treatment. *Journal of Materials Engineering and Performance*, 2002, 11(1): 19-25.
- [12] K Harris, J B Wahl. Improved single crystal superalloy, CMSX-4 (R)(SLS)[La+Y] and CMSX-486 (R). In: Green KA, Pollock TM, Harada H, Howson TE, Reed RC, Schirra JJ, et al. (eds). *Superalloy 2004*. Warrendale: Minerals, Metals & Materials Soc, 2004: 45-52.
- [13] M G Wang, S G Tian, X F Yu, et al. Effects of heat treatment on composition segregation and enduring properties of single crystal nickel-based superalloy[J]. *Journal of Shenyang University of Technology*, 2009, 31(6): 525-530.